Indian Journal of Chemistry
Vol. 65, February 2026, pp. 91-103
DOI: 10.56042/ijc.v65i2.18758

New fused imidazo-pyrimidine and imidazo-purine derived from maleimide and nucleobases: One pot synthesis, structure elucidation, antioxidant and antimicrobial evaluation

Rabia Youmbai[a], Nawal Khier[b], Mohamed Dehamchia*[a], Samir Bayou[c] & Zine Régaïnia[d]

[a] Laboratory of Applied Chemistry and Environment, Department of Chemistry, University of El Oued, PO Box 789, 39000, Algeria

[b] Laboratory of Bioinformatics, Applied Microbiology and Biomolecules, University of Boumerdès, 35000 Bumerdès, Algeria

[c] Laboratory of Macromolecular Synthesis and Thio-Organic Macromolecular (LSMTM), Department of Macromolecular Chemistry, Faculty of Chemistry, USTHB BP 32 el Alia, Algiers, 16111, Algeria

[d] Laboratory of Applied Organic Chemistry (LAOC), Faculty of Sciences, Department of Chemistry, Badji Mokhtar University PO Box 12 Annaba-Algeria

E-mail: mohchar5@yahoo.fr, dehamchia-mohamed@univ-eloued.dz

Received 11 April 2025; accepted (revised) 30 January 2026

A series of novel quinoxalinones, (2,5-dioxoimidazo[1,2-f]pyrimidin-3-yl)acetamide, 8-oxo-3*H*-imidazo[1,2-g]purin-7-yl)acetamide, and 4,7-dioxo-3H-imidazo[2,1-e]purin-8-yl)acetamide, were synthesized by reaction of maleimide derivatives with substituted *ortho*-phenylenediamine or nucleobases. The analytical methods such as FT-IR, ^{1}H and ^{13}C NMR spectroscopy, mass spectrometry, and microanalyses (C, H, N) were utilized to elucidate the structures of the target compounds. These products were tested for their ability to scavenge DPPH$^{\bullet}$ (1,1-diphenyl-1-picrylhydrazyl) and ABTS$^{+\bullet}$ (2,2′-azino-bis(3-ethylbenzothiazoline-6-sulfonic acid) free radicals, as well as for their total antioxidant capacity (TAC). Additionally, antimicrobial activity was screened against four bacterial strains and fungi using the well diffusion method. The results demonstrated that quinoxalinone **1f** exhibited potent free radical scavenging activities against DPPH and ABTS radicals, with IC_{50} values of 1.67 µg mL^{-1} and 20.76 µg mL^{-1}, respectively, compared to the standard antioxidant ascorbic acid (IC_{50} values of 2.82 and 74.22 µg mL^{-1}, respectively). Compound **1f** also displayed the highest TAC with a value of 1303 mg (AAE)/g of dry compound. Furthermore, (2,5-dioxoimidazo[1,2-f]pyrimidin-3-yl)acetamide (**2a**) demonstrated superior antioxidant activity against ABTS radical, with an IC_{50} value of 73.89 µg mL^{-1}, which is lower than that of the ascorbic acid (74.22 µg mL^{-1}). The antimicrobial assay revealed that compound **1f** exhibited potent inhibitory effects against all tested bacterial and fungal strains.

Keywords: Quinoxaline, Imidazole, Nucleobases, Antioxidant activity, Antimicrobial activity

Recent research has been enriched by novel discoveries in the synthesis and the biological evaluation of nitrogen-containing heterocycles. These compounds are of great interest due to their widespread presence in diverse synthetic materials[1,2] and bioactive molecules[3].

Among these, imidazoles stand out as a significant class of *N*-heterocyclic compounds. They have garnered considerable attention for their extensive range of biological potentials, including anticancer[4], antibacterial[5], anti-inflammatory[6], antiviral[7], anti-histaminic[8], antiparasitic[9], antitubercular[10], anti-malarial[11], antidaibetic[12], antineuropathic[13], anti-obesity[14], and antihypertensive[15] activities. Additionally, pyrimidine and purine molecules play a pivotal role in organic synthesis, particularly in medicinal chemistry. These structures are fundamental components of physiologically important compounds such as DNA and RNA[16,17]. The imidazole ring itself is a key feature in many bioactive compounds[18,19].

Fused imidazo-pyrimidine and imidazo-purine derivatives exhibit an even broader spectrum of therapeutic activities, including anticancer[20,21], antimicrobial[22-24], anti-inflammatory[25,26], antiviral[27-29], anticonvulsant[30-32], antidepressant[33,34], antioxidant[22], antimalarial[35,36], and antidiabetic[37] effects.

In recent years, numerous methods have been developed for synthesizing of imidazole, imidazo-pyrimidine and imidazo-purine derivatives. These include microwave-assisted techniques[38,39], multi-component reactions (MCRs)[20,40-42], catalyst-free reactions, and green synthesis approaches[43-46]. The emergence of antimicrobial resistance has become a

critical global health challenge. Its alarming increase has led to higher morbidity, mortality, and healthcare costs, while rendering many conventional antibiotics ineffective. This growing crisis highlights the urgent need for new antibacterial agents capable of combating resistant pathogens. Nitrogen-containing heterocyclic compounds have gained significant attention in medicinal chemistry due to their structural diversity and proven bioactivity. These compounds offer valuable scaffolds for developing innovative antimicrobial therapies[24,47,48]. The synthesized compounds in this study demonstrate potent antibacterial and antifungal activity, providing critical insights into the development of next-generation antimicrobials to address resistant infections.

Given the therapeutic potential of imidazole and its fused derivatives, the synthesis of novel fused imidazo-pyrimidine and imidazo-purine compounds has captured our interest[49]. This study aims to synthesize new fused imidazo-pyrimidines and imidazo- purines derivatives and to and to assess their potential antioxidant and antimicrobial activities.

The antioxidant potentials against free radicals of these compounds were measured trough DPPH, ABTS, and TAC assays, while their antimicrobial activities were examined trough the well-diffusion method.

Experimental Section

Melting Point Apparatus 240 VAC and are reported as uncorrected values. The ^{1}H and ^{13}C NMR spectra of the target compounds were recorded at RT on a Bruker Avance spectrometer. High-resolution mass spectra (HRMS-ESI) were obtained using a Waters Micromass AutoSpec-Ultima spectrometer equipped with a direct inlet probe operating at 70 eV. The IR spectra (in KBr, $\bar{\upsilon}$ cm^{-1}) were run on Agilent Cary 630 FT-IR spectrometer. Elemental (C, H, N) microanalyses were performed using a Carlo Erba EA 1108 apparatus**.** Melting points (mp.) were determined using a Cole-Parmer MP-200D Stuart Digital Absorbance measurements for the antioxidant assays were conducted using Secomam Prim Light spectrophotometer. TLC was carried out with Silica Gel 60Å F254 precoated plates. All reagents and solvents were obtained from commercial sources and were used as received unless otherwise indicated.

Chemical synthesis

Synthetic procedure of quinoxalines (1a-d) [50]

These compounds were synthesized according to a previously reported procedure[50].

Typical procedure for the synthesis of quinoxalines, 1e-k

Equimolar quantities of *N*-substituted maleimide (2 mmol) and substituted *o*-phenylenediamine (2 mmol) were mixed in ethanol (20 mL) and was heated at reflux (90°C) for 24 hours. After completion, the reaction mixture was cooled to RT, and an excess amount of ice water was added. The solid which formed was filtered off was purified by recrystallization from ethanol at low temperature.

1e: It was synthesized using *N*-methylmaleimide (0.22g, 2 mmol) and 4-nitro-*o*-phenylenediamine (0.31g, 2 mmol) in EtOH. Red solid. Yield 42%. m.p.192-194°C. FT-IR (KBr): 3428(NHC=O), 3376 ($NHCH_3$), 3324(NH), 1743 (C=O), 1626 (C=O), 1460 (N-O) 1230 cm^{-1} (N-O); ^{1}H NMR (400 MHz, DMSO-d_6): δ 8.43 (s, 1H, NHC=O), 7.58 (s, 1H, CH_{arom}), 7.18 (d, *J*= 2.6 Hz, 1H, CH_{arom}), 7.00 (s, 1H, $NHCH_3$), 6.72 (d, *J*= 8.5 Hz, 1H, CH_{arom}), 6.31 (s, 1H, NH), 4.33 (t, *J*= 5.0 Hz, 1H, CH_{ethyl}), 2.86 (s, 3H, CH_3), 2.72 (dd, *J*= 9.4, 4.9 Hz, 1H, H_aCH_b), 2.31 (dd, *J*= 9.4, 4.9 Hz, 1H, H_aCH_b); HRMS (ESI): *m/z* 265.0929 $[M+H]^+$ (Calcd for $[C_{11}H_{12}N_4O_4+H]^+$=265.0937). Anal. Calcd for $C_{11}H_{12}N_4O_4$ (264.24 g mol^{-1}): C, 50.00; H, 4.58; N, 21.20. Found: C, 50.06; H, 4.81; N, 21.12%.

2-(6,7-Dichloro-3-oxo-1,2,3,4-tetrahydroquinoxalin-2-yl)-N-methylacetamide, 1f: It was synthesized using *N*-methylmaleimide (0.22g, 2 mmol) and 4,5-dichloro-*o*-phenylenediamine (0.35g, 2 mmol) in EtOH. Brown solid. Yield 45%. m.p.210-212°C. FT-IR (KBr): 3391(NHC=O), 3370($NHCH_3$), 3316(NH), 1744 (C=O), 1639 (C=O), 670 (C-Cl), 612 cm^{-1} (C-Cl); ^{1}H NMR (600 MHz, DMSO-d_6): δ 10.49 (s, 1H, NHC=O), 7.24 (s, 1H, CH_{arom}), 7.09 (s, 1H, $NHCH_3$), 7.00 (s, 1H, CH_{arom}), 6.93 (s, 1H, NH), 4.06 (t, *J* = 5.0 Hz, 1H, CH_{ethyl}), 2.99 (dd, *J* = 9.5, 4.8 Hz, 1H, H_aCH_b), 2.78 (dd, *J* = 9.5, 4.8 Hz, 1H, H_aCH_b), 2.08 (s, 3H, CH_3); HRMS (ESI): *m/z*288.2289 $[M+H]^+$ (Calcd for $[C_{11}H_{11}Cl_2N_3O_2+H]^+$= 288.0306). Anal. Calcd for $C_{11}H_{11}Cl_2N_3O_2$ (288.10 g mol^{-1}): C, 45.85; H, 3.85; N, 14.58. Found: C, 49.19; H, 3.46; N, 14.17%.

1g: It was synthesized using *N*-methylmaleimide (0.22g, 2 mmol) and 4-methyl-*o*-phenylenediamine (0.24g, 2 mmol) in EtOH. Brown solid. Yield 40%. m.p.216-218°C. FT-IR (KBr): 3400(NHC=O), 3360($NHCH_3$), 3200(NH), 2928 (C-H_{SP^3}), 1676 (C=O), 1632 cm^{-1} (C=O); ^{1}H NMR (400 MHz, DMSO-d_6): δ

8.15 (s, 1H, NHC=O), 7.39 (s, 1H, N*H*CH_3), 7.13 – 6.94 (m, 3H, CH_{arom}), 6.01 (s, 1H, NH), 3.50 (t, *J* = 5.0 Hz, 1H, CH_{ethyl}), 3.18 (dd, *J* = 9.6, 4.5 Hz, 1H, H_aCH_b), 2.93 (dd, *J* = 9.6, 4.5 Hz, 1H, H_aCH_b), 2.67 (s, 3H, NHCH_3), 1.23 (s, 3H, CH_3); HRMS (ESI): *m/z*234.1252 $[M+H]^+$ (Calcd for $[C_{12}H_{15}N_3O_2+H]^+$=234.1242). Anal. Calcd for $C_{12}H_{15}N_3O_2$ (233.25 g mol^{-1}): C, 61.79; H, 6.48; N, 18.01. Found: C, 61.77; H, 5.8; N, 18.36%.

2-(3-Oxo-1,2,3,4-tetrahydroquinoxalin-2-yl)-N-phenylacetamide, 1h[51]: It was prepared using *N*-phenylmaleimide (0.35g, 2 mmol) and *o*-phenylenediamine (0.36g, 2 mmol) in EtOH. Yellow solid. Yield 69%. m.p.225-226°C. FT-IR (KBr): 3370(NHPh), 3288(NHC=O), 3197 (NH), 1677 (C=O), 1647 cm^{-1} (C=O); ^{1}H NMR (400 MHz, DMSO-d_6): δ 10.29 (s, 1H, NHC=O), 10.00 (s, 1H, NHPh), 7.61 (d, *J* = 7.3 Hz, 2H, CH_{arom}), 7.32 – 7.27 (m, 2H, CH_{arom}), 7.04 (t, *J* = 7.4 Hz, 1H, CH_{arom}), 6.78 – 6.74 (m, 3H, CH_{arom}), 6.62 (d, *J* = 2.6 Hz, 1H, CH_{arom}), 5.97 (s, 1H, NH), 4.25 – 4.19 (m, 1H, CH_{ethyl}), 2.90 (dd, *J* = 15.4, 4.6 Hz, 1H, H_aCH_b), 2.61 (dd, *J* = 15.4, 8.0 Hz, 1H, H_aCH_b); ^{13}C NMR (101 MHz, DMSO-d_6): δ 168.93 (C=O), 167.42 (C=O), 139.62 (C_{arom}), 134.37 (C_{arom}), 129.11 (CH_{arom}), 126.43 (C_{arom}), 123.62 (CH_{arom}), 123.27 (CH_{arom}), 119.65 (CH_{arom}), 118.51 (CH_{arom}), 115.28 (CH_{arom}), 114.31 (CH_{arom}), 53.11 (CH_{ethyl}), 39.12 (CH_2); HRMS (ESI): *m/z* 282.1242 $[M+H]^+$ (Calcd for $[C_{16}H_{15}N_3O_2+H]^+$: 282.1243). Anal. Calcd for $C_{16}H_{15}N_3O_2$ (281.29 g mol^{-1}): C, 68.31; H, 5.37; N, 14.94. Found: C, 68.17; H, 5.62; N, 14.68%.

1i: It was synthesized using *N*-phenylmaleimide (0.35g, 2 mmol) and 4-chloro-*o*-phenylenediamine (0.27g, 2 mmol) in EtOH. Brown solid. Yield 42%. m.p.130-132°C. FT-IR (KBr): 3280(NHPh), 3194(NHC=O), 3135(NH), 1706(C=O), 1669(C=O), 751 cm^{-1} (C-Cl); ^{1}H NMR (600 MHz, DMSO-d_6): δ 10.62 (s, 1H, NHC=O), 10.44 (s, 1H, N*H*Ph), 7.77 (d, *J* = 8.4 Hz, 1H, CH_{arom}), 7.67 – 7.60 (m, 2H, CH_{arom}), 7.49 (s, 1H, NH), 7.46 – 7.38 (m, 2H, CH_{arom}), 7.09 – 6.99 (m, 1H, CH_{arom}), 6.66 – 6.58 (m, 1H, CH_{arom}), 5.90 (s, 1H, CH_{arom}), 4.27 – 4.20 (m, 1H, CH_{ethyl}), 3.10 (dd, *J* = 15.7, 4.0 Hz, 1H, H_aCH_b), 2.95 (dd, *J* = 15.7, 8.4 Hz, 1H, H_aCH_b); HRMS (ESI): *m/z* 316.0861$[M+H]^+$ (Calcd for [for $C_{16}H_{14}ClN_3O_2+H]^+$: 316.0852). Anal. Calcd for $C_{16}H_{14}ClN_3O_2$ (315.73 g mol^{-1}): C, 60.86; H, 4.47; N, 13.31. Found: C, 60.87; H, 4.72; N, 13.02%.

1j: It was synthesized using *N*-phenylmaleimide (0.35g, 2 mmol) and 4-nitro-*o*-phenylenediamine (0.31g, 2 mmol) in EtOH. Red solid. Yield 50%. m.p.222-224°C. FT-IR (KBr): 3432(NHPh), 3379(NHC=O), 3327(NH), 1657 (C=O), 1636 (C=O), 1470 (N-O), 1259 cm^{-1} (N-O); ^{1}H NMR (400 MHz, DMSO-d_6): δ 10.85 (s, 1H, NHC=O), 10.01 (s, 1H, N*H*Ph), 7.90 (d, *J* = 7.8 Hz, 1H, CH_{arom}), 7.72 (d, *J* = 8.7 Hz, 1H, CH_{arom}), 7.66 – 7.57 (m, 5H, CH_{arom}), 6.90 (s, 1H, NH), 6.33 (d, *J* = 8.4 Hz, 1H, CH_{arom}), 4.37 – 4.25 (m, 1H, CH_{ethyl}), 2.99 (dd, *J* = 15.3, 4.9 Hz, 1H, H_aCH_b), 2.88 (dd, *J* = 15.3, 8.1 Hz, 1H, H_aCH_b); HRMS (ESI): *m/z* 327.1022 $[M+H]^+$ (Calcd for [for $C_{16}H_{14}N_4O_4+H]^+$: 327.1093). Anal. Calcd for $C_{16}H_{14}N_4O_4$ (326.29 g mol^{-1}): C, 58.89; H, 4.32; N, 17.17. Found: C, 59.20; H, 4.52; N, 16.92%.

1k: It was synthesized using *N*-phenylmaleimide (0.35g, 2 mmol) and 4-methyl-*o*-phenylenediamine (0.24g, 2 mmol) in EtOH. Yellow solid. Yield 64%. m.p.198-200°C. FT-IR (KBr): 3372(NHPh), 3289(NHC=O), 3189(NH), 2919(C-H_{SP^3}), 1672(C=O), 1654 cm^{-1} (C=O); ^{1}H NMR (600 MHz, DMSO-d_6): δ 10.26 (s, 1H, NHC=O), 10.22 (s, 1H, NHPh), 7.67 (s, 1H, CH_{arom}), 7.59 (d, *J* = 8.0 Hz, 2H, CH_{arom}), 7.49 (s, 1H, NH), 7.03 (t, *J* = 7.6 Hz, 2H, CH_{arom}), 6.68 – 6.58 (m, 1H, CH_{arom}), 6.45 – 6.41 (m, 1H, CH_{arom}), 5.84 (s, 1H, CH_{arom}), 4.18 – 4.13 (m, 1H, CH_{ethyl}), 2.83 (dd, *J* = 15.3, 4.1 Hz, 1H, H_aCH_b), 2.58 (dd, *J* = 15.3, 8.6 Hz, 1H, H_aCH_b), 2.15 (s, 3H, CH_3); HRMS (ESI^+): *m/z* 295.1391 $[M+H]^+$ (Calcd for [for $C_{17}H_{17}N_3O_2+H]^+$: 296.1399). Anal. Calcd for $C_{17}H_{17}N_3O_2$ (295.31 g mol^{-1}): C, 69.13; H, 5.80; N, 14.23. Found: C, 69.30; H, 5.65; N, 14.10%.

Synthetic procedure for the preparation of fused imidazo-pyrimidines 2a and imidazo-purines, 3a and 4a

An equimolar quantities of maleimide (2 mmol) and nucleobase (cytosine, adenine, or guanine) **(**2 mmol**)** were mixed in ethanol (20 mL) and stirred at reflux for 24 h. TLC was utilized to monitor the progress of the reaction. After completion, the mixture was cooled to RT, and an excess of ice water was added. The desired product was achieved by vacuum filtration and subsequently purified by recrystallization from ethanol.

2-(2,5-Dioxo-2,3,5,6-tetrahydroimidazo[1,2-c]pyrimidin-3-yl)acetamide, 2a: It was synthesized using maleimide (0.22g, 2 mmol) and cytosine (0.25g, 2

mmol) in EtOH. White solid. Yield 52%. m.p.269-271°C. FT-IR (KBr): 3422$(NH_2)_{amide}$, 3322 $(NH)_{amide}$, 1715$(C=O)_{amide}$, 1652$(C=O)_{amide}$, 1640 cm^{-1} $(C=O)_{amide}$; ^1H NMR (400 MHz, DMSO-d_6): δ 11.28 (s, 1H, NH), 7.60 (d, J = 7.3 Hz, 1H, $NHCH_{pyrimidine}$), 7.24 (s, 2H, NH_2), 5.70 (d, J = 7.2 Hz, 1H, $CH_{pyrimidine}$), 4.81 (dd, J = 8.7, 5.4 Hz, 1H, $CH_{imidazole}$), 2.91 (dd, J = 17.6, 8.1 Hz, 1H, H_aCH_b), 2.75 (dd, J = 17.6, 5.4 Hz, 1H. H_aCH_b); ^{13}C NMR (101 MHz, DMSO-d_6): δ 168.93 (C=O), 167.42 (C=O), 139.62 (C_{arom}), 134.37 (C_{arom}), 129.11 (CH_{arom}), 126.43 (C_{arom}), 123.62 (CH_{arom}), 123.27 (CH_{arom}), 119.65 (CH_{arom}), 118.51 (CH_{arom}), 115.28 (CH_{arom}), 114.31 (CH_{arom}), 53.11 (CH_{ethyl}), 39.12 (CH_2); HRMS (ESI^+): *m/z* 209.0673 $[M+H]^+$ (Calcd for $[C_8H_8N_4O_3+H]^+$: 209.0669). Anal. Calcd for $C_8H_8N_4O_3$ (208.17 g mol^{-1}): C, 46.15; H, 3.87; N, 26.91. Found: C, 46.16; H, 3.96; N, 26.73%.

2-(7,8-Dihydro-8-oxo-3*H*-imidazo[2,1-i]purin-7-yl)acetamide, 3a: It was synthesized using maleimide (0.19g, 2 mmol) and adenine (0.27g, 2 mmol) in EtOH. Pink solid. Yield 76%. m.p.165-167°C. FT-IR (KBr): 3370$(NH_2)_{amide}$, 3161$(NH)_{amine}$, 1685$(C=O)_{amide}$, 1625 cm^{-1} (C=O); ^1H NMR (600 MHz, DMSO-d_6): δ 9.52 (d, J = 14.4 Hz, 1H, N*H*), 8.91 (s, 1H, NHCH_{purine}), 8.50 (d, J = 7.7 Hz, 1H, CH_{purine}), 7.96 (d, J = 5.1 Hz, 1H, H_cNH_d), 7.56 (d, J = 5.2 Hz, 1H, H_cNH_d), 5.49 (t, J = 7.8 Hz, 1H, C$H_{imidazole}$), 3.28 (dd, J = 14.8, 7.8 Hz, 1H, H_aCH_b), 3.15 (dd, J = 14.7, 7.8 Hz, 1H, H_aCH_b); HRMS (ESI^+): *m/z* 233.0791 $[M+H]^+$ (Calcd for $[C_9H_8N_6O_2+H]^+$: 233.0792). Anal. Calcd for $C_9H_8N_6O_2$ (232.20 g mol^{-1}): C, 46.55; H, 3.47; N, 36.19. Found: C, 46.51; H, 3.44; N, 36.12%.

2-(4,5,7,8-Tetrahydro-4,7-dioxo-3*H*-imidazo[2,1-b]purin-8-yl)acetamide, 4a: It was synthesized using maleimide (0.16g, 2 mmol) and guanine (0.25g, 2 mmol) in EtOH. Brown solid. Yield 49%. m.p.284-287°C. FT-IR (KBr): 3316$(NH)_{amide}$, 3117$(NH_2)_{amide}$, 3000 $(NH)_{amine}$,1690$(C=O)_{amide}$, 1672$(C=O)_{amide}$, 1640 cm^{-1} $(C=O)_{amide}$; ^1H NMR (600 MHz, DMSO-d_6): δ 8.11 (d, J = 7.3 Hz, 1H, NH_{purine}), 7.76 (s, 1H, NH_{purine}), 7.63 (d, J = 7.8 Hz, 1H, CH_{purine}), 6.86 (d, J = 4.2 Hz, 1H, H_cNH_d), 6.64 (d, J = 8.4 Hz, 1H, H_cNH_d), 5.32 (t, J = 5.0 Hz, 1H, $CH_{imidazole}$), 2.38 (dd, J = 12.8, 5.0 Hz, 1H, H_aCH_b), 2.20 (dd, J = 12.7, 5.0 Hz, 1H, H_aCH_b); HRMS (ESI^+): *m/z* 249.0732 $[M+H]^+$ (Calcd for $[C_9H_8N_6O_3+H]^+$: 249.0736). Anal. Calcd for $C_9H_8N_6O_3$ (248.20): C, 43.55; H, 3.25; N, 33.86. Found: C, 43.52; H, 3.22; N, 33.83%.

Biological evaluation

Antioxidant activity

The *in vitro* antioxidant properties of the quinoxalinones (**1a-k**), (2,5-dioxoimidazo[1,2-f]pyrimidin-3-yl) acetamide **(2a)**, (8-oxo-3H-imidazo[1,2-g]purin-7-yl)acetamide **(3a)**, and (4,7-dioxo-3H-imidazo[2,1-e]purin-8-yl)acetamide **(4a)** were evaluated using several methods. These included the $DPPH^{\bullet}$ and $ABTS^{\bullet+}$ radical quenching assay, and the TAC method.

DPPH radical quenching assay [52]

Briefly, 1 mL of each synthesized compounds and the standard antioxidant (ascorbic acid) were prepared at different concentrations (from 2.5 to 125 μg mL^{-1}). These solutions were then mixed with 1 mL of a 2 mM DPPH solution and stirred thoroughly. After incubation in the dark conditions for 30 minutes, the absorbance of the mixture was recorded at a wavelength of 517 nm.

The percentage inhibition of DPPH radicals was calculated using the following formula:

$$\% \text{ Inhibition } = \left[\frac{Abs_{control} - Abs_{sample}}{Abs_{control}}\right] \times 100$$

Where:

$Abs_{control}$ is the DPPH radical absorbance and Abs_{sample} is the absorbance of the tested sample.

The results of the DPPH radical scavenging activity were expressed as percentage inhibition and IC_{50} values, which represents the inhibitory concentration of the tested sample needed to quench 50% of the $DPPH^{\bullet}$. The obtained results are presented in Table 1 and depicted in Fig. 1.

ABTS radical quenching assay

The ABTS radical scavenging activity of the synthesized products was also investigated[53]. Solutions of the tested compounds were prepared at different concentrations (from 2.5 to 125 μg mL^{-1}) in 1 mL volumes. The ABTS radical solution was generated by reacting 2.4 mM ABTS with 70 mM potassium persulfate in water. This solution was left to stand in the dark for 12–16 hours to ensure complete oxidation and stabilization of the $ABTS^{\bullet+}$ radical. After dilution with methanol, the absorbance was measured at wavelength of around 734 nm.

Next, 990 μL of the diluted $ABTS^{\bullet+}$ solution was mixed with 10 μL of the tested compounds at various concentrations and allowed to react for 7 minutes in the

Table 1 — DPPH radical scavenging activity of **1a-k**, **2a**, **3a** and **4a**

Compd	Concentration (µg mL^{-1})							
	2.5	12.5	25	37.5	50	62.5	75	IC_{50}
1a	47.05	76.13	84.02	90.68	95.12	95.78	96.89	8.72
1b	51.61	65.81	67.81	80.68	86.57	90.34	90.89	14.36
1c	51.27	66.25	72.91	82.90	86.24	88.68	89.90	13.23
1d	64.08	73.87	80.68	87.48	91.97	94.55	94.82	5.02
1e	59.04	66.39	68.57	70.06	71.56	73.06	73.6	14.49
1f	70.28	80.28	80.71	81	82.28	84	84.14	1.67
1g	50.34	67.48	71.42	71.83	77	78.36	83.67	15.67
1h	70.88	73.33	74.69	90.06	94.96	95.64	95.91	3.75
1i	42.17	58.23	73.46	79.72	83.12	85.3	87.07	17.69
1j	51.97	74.55	79.45	82.17	83.8	84.35	86.39	9.39
1k	48.16	76.19	82.44	88.43	91.97	92.92	92.92	8.80
2a	60.05	58.57	56.83	49.46	48.25	45.84	38.47	–
3a	65.14	64.83	64.51	63.72	60.88	58.20	48.58	–
4a	58.71	54.42	41.82	39.27	32.70	26.27	9.38	–
Vit C	72.70	72.92	75.25	75.80	77.14	79.69	80.91	2.82

(–): No activity observed

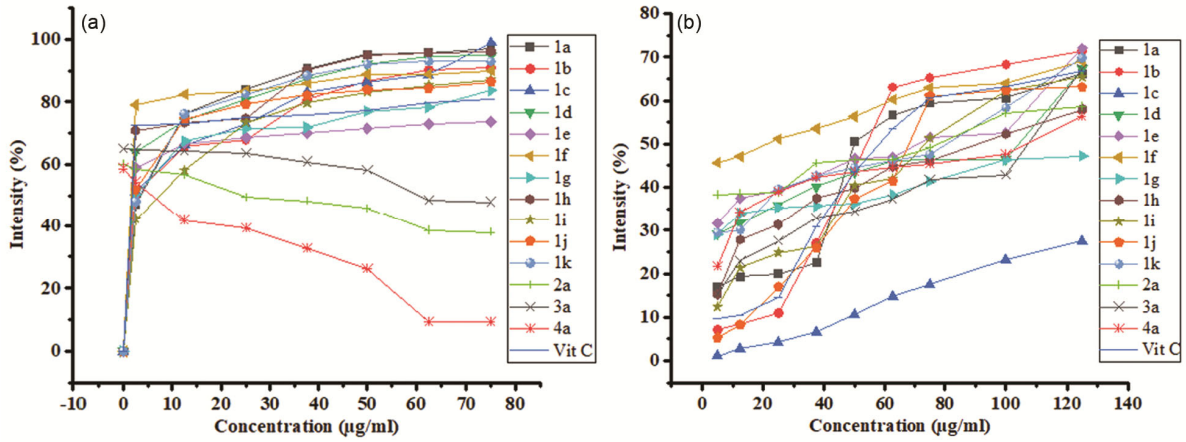

Fig. 1 — DPPH$^{\bullet}$ (A) and ABTS$^{+\bullet}$ (B) quenching capacity as a function of different concentrations of quinoxalinones **(1a-k)**, imidazo-pyrimidine **2a**, imidazo-purines(**3a** and **4a**)

dark. Ascorbic acid was used as the positive control. The absorbance was recorded at a wavelength of 734 nm. The percentage of antioxidant effectiveness against ABTS$^{\bullet+}$ radicals was calculated using the formula:

$$\%\ Inhibition = \left[\frac{Abs_{control} - Abs_{sample}}{Abs_{control}}\right] \times 100$$

Where:

$Abs_{control}$ is the ABTS radical absorbance and Abs_{sample} is the absorbance of the tested sample.

The results of the ABTS radical scavenging activity were expressed as percentage inhibition and IC_{50} values. The results are summarized in Table 2 and illustrated in Fig. 1.

Total antioxidant capacity (TAC)

The TAC of the prepared compounds was assessed using the phosphomolybdate technique[54]. This assay measures the TAC by quantifying the reduction of Mo (VI) to green Mo (V) by the antioxidant compounds under acidic *p*H conditions. Briefly, 0.2 mL of each compound (at a concentration of 62.5 µg mL^{-1}) was mixed with 2 mL of a specific reagent solution containing 0.6 M sulfuric acid, 28 mM sodium phosphate, and 4 mM ammonium molybdate. After incubation at 95°C for 90 minutes, the reaction mixture was allowed to cool to RT. The absorbance of each sample was measured at a wavelength of 695, which is the maximum absorption for the green phosphomolybdenum complex.

Table 2 — ABTS radical scavenging activity of **1a-f**, **2a**, **3a** and **4a**

Compd	Concentration (μg mL^{-1})									
	5	12.5	25	37.5	50	62.5	75	100	125	IC_{50}
1a	16.94	19.31	22.08	39.31	50.51	55	59.31	63.75	66.11	68.67
1b	7.22	8.33	10.97	26.94	44.31	63.05	65.28	68.33	71.38	69.43
1c	1.11	2.78	4.31	6.67	10.69	14.72	17.50	23.19	27.50	218.89
1d	29.14	31.71	35.86	40.14	43.29	46	46.42	46.43	67.28	81.78
1e	31.65	37.39	39.35	42.58	46.64	46.92	51.54	52.52	71.99	66.54
1f	45.65	47.05	51.12	53.50	56.30	60.22	62.88	63.86	68.90	20.76
1g	29.03	33.88	35.27	35.55	36.11	38.33	41.38	46.25	47.22	137.95
1h	15.20	27.84	31.25	37.36	39.77	44.74	46	52.27	57.95	89.50
1i	12.38	21.28	24.76	26.27	40.47	42	51.32	62.03	65.37	80.15
1j	5.39	8.23	16.88	26.01	37.30	41.42	61	62.41	63.12	80.72
1k	29.43	30.14	39.57	42.56	44.57	46.14	47.57	58.29	69.71	69.77
2a	38.19	38.47	38.76	45.54	46.25	46.39	49.08	57	58.58	73.89
3a	15.43	22.86	27.57	32.86	34.43	37.14	41.86	42.86	67.14	95.35
4a	21.64	34.23	39.04	42.29	43.56	44.70	45.26	47.67	56.29	93.83
Vit C	9.78	10.46	14.54	30.84	43.61	53.40	60.73	63.18	66.85	74.22

The TAC of the samples was expressed in terms of ascorbic acid equivalents (AAE).
[$A=4.5483x+0.0065$; $R^2= 0.9958$]
Where:
A = Absorbance at 695 nm.
x = Concentration of AAE (mg AAE/g of dry compound).

The TAC values were measured in terms of ascorbic acid equivalents, using the calibration curve equation $y=4.5483x+0.0065y=4.5483x+0.0065$, at a concentration of 0.0625 μg mL^{-1}. The results of the TAC assessment for the evaluated compounds are depicted in Fig. 2.

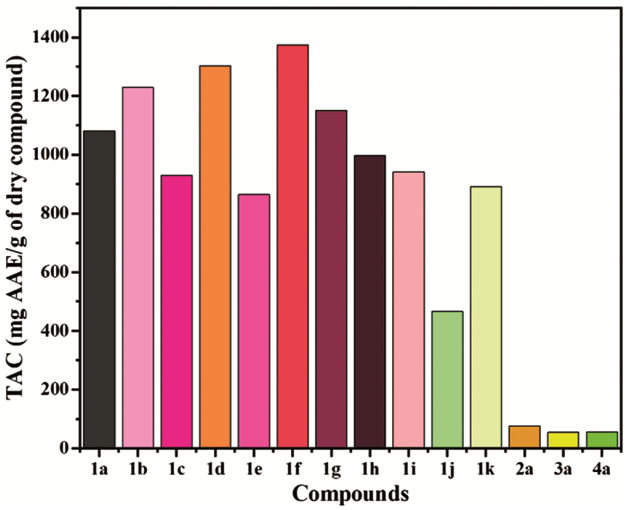

Fig. 2 — TAC of **1a-f**, **2a**, **3a** and **4a** measured by phosphomolybdenum method

Antimicrobial activity

The antimicrobial activity of the compounds was evaluated using the well-diffusion method[55]. Muller-Hinton agar was prepared for bacterial cultures, while Sabouraud dextrose agar was used for yeast cultures. The agar media were poured into sterile Petri dishes and allowed to solidify. Wells were then created in the agar, and bacterial or yeast suspensions were inoculated onto the surface. A volume of 60 μL of each tested sample was added to the wells.

The plates were incubated at 37°C for 24 hours (for bacterial growth) or 48 hours (for yeast growth) to allow for microbial proliferation and agent diffusion. Following incubation, the diameter of the zone of inhibition (ZOI) was measured and the results are presented in Table 3. Gentamicin and nystatin were used as positive controls for antibacterial and antifungal tests, respectively, while DMSO served as the negative control.

Results and Discussion

Chemistry

As described in a previous study, the condensation of *N*-substituted maleimide with substituted *o*-phenylenediamine in EtOH resulted in the formation of quinoxalinone derivatives **(1a-k)** (Scheme 1)[50]. All compounds were produced in moderated to good yields (40%-80%), and the detailed results are presented in Table 4.

Furthermore, we explored the synthesis of novel fused imidazo-pyrimidine **2a** and imidazo-purine compounds (**3a** and **4a**), as detailed in Scheme 1. This approach involved replacing of *o*-phenylendiamines

Table 3 — ZOI in mm of the tested compounds

	Diameter of inhibition zones (mm)				
Compd	*E. coli*	*K. pneumoniae*	*P. aeruginosa*	*S. aureus*	*C. albicans*
1a	14	12	–	–	9
1b	11	10	–	–	7
1c	10	8	–	–	10
1d	–	–	9	–	10
1e	–	12	9	13	13
1f	19	17	11	20	20
1h	14	14	8	13	9
1j	9	11	8	9	10
1k	–	11	7	10	10
2a	–	11	–	–	–
3a	–	–	–	–	–
4a	–	–	–	–	–
Gentamicin	22	20	19	21	–
Nystatin	–	–	–	–	24

(–): No activity was observed

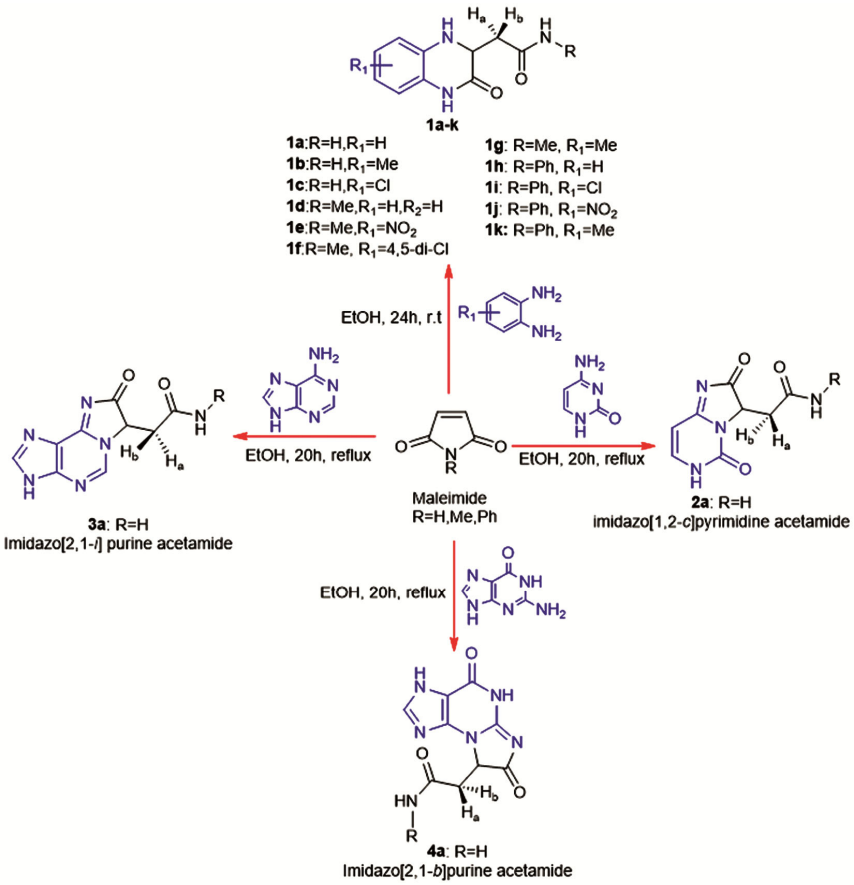

Scheme 1 — The synthesis routes for the preparation of quinoxalinones, fused imidazo-pyrimidine, and imidazo-purine derivatives

with nitrogenous bases (nucleobases), such as cytosine, adenine, and guanine, which act as 1,3-diamines due to the presence of an amino (NH_2) group.

An ethanolic solution containing maleimide and nucleobases (cytosine, adenine or guanine) was refluxed for 24 h until the entire starting materials were fully consumed, as confirmed by TLC analysis.

Table 4 — Structure characterization and yields of synthesized quinoxalinones **(1a-k)** compounds

Product	Yield(%)	Ref. No.	m.p. (°C)
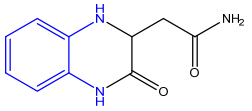 **1a**	80[a]	50	278-280
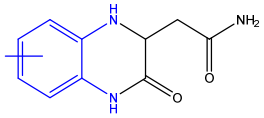 **1b**	70[a]	50	258-260
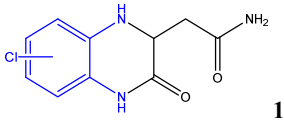 **1c**	60[a]	50	180-183
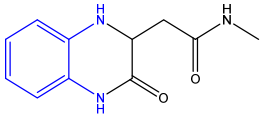 **1d**	70[a]	50	194-196
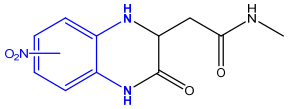 **1e**	42[b]	–	192-194
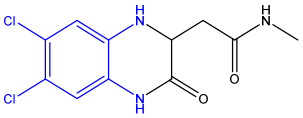 **1f**	45[b]	–	210-212
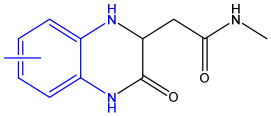 **1g**	40[b]	–	216-128
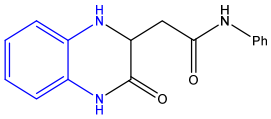 **1h**	69[b]	51	225-227
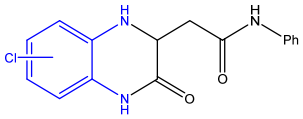 **1i**	42[b]	–	130-132
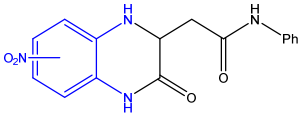 **1j**	50[b]	–	222-224
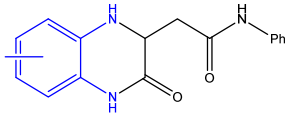 **1k**	64[b]	–	198-200

[a]: EtOH, 24 h, RT; [b]: EtOH, 20 h, reflux

The resulting solids were then isolated *via* vacuum filtration to yield pure products in moderated yields (49%-76%), as shown in Table 5. Among this, 2-(7,8-dihydro-8-oxo-3*H*-imidazo[1,2-g]purin-7-yl)acetamide (**3a**) exhibited the highest yield (76%) when adenine was used as the starting materials. This higher yield can be attributed to the absence of the carbonyl group (C=O) in the structure of adenine, which likely facilitated the reaction efficiency.

Table 5 — Structure characterization and yields of synthesized imidazo-pyrimidine **2a** and imidazo-purines (**3a** and **4a**)

Product	Nucleobase	Yield(%)	m.p. (°C)
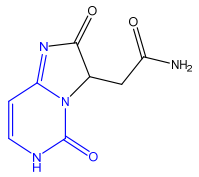 **2a**	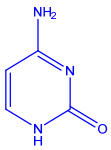	52[(b)]	269-271
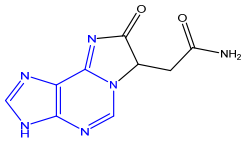 **3a**	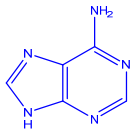	76[(b)]	165-167
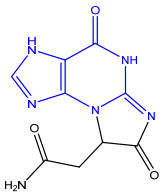 **4a**	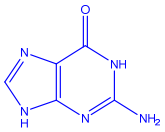	49[(b)]	284-287

[(b)]: EtOH, 24h, reflux

The structures of (2,5-dioxoimidazo[1,2-f]pyrimidin-3-yl) acetamide (**2a**), 8-oxo-3*H*-imidazo[1,2-g]purin-7-yl)acetamide (**3a**) and 4,7-dioxo-3H-imidazo[2,1-e]purin-8-yl)acetamide (**4a**) were determined using their spectral data (^{1}H- and ^{13}C NMR, FT-IR and ESI-MS) and Elemental (C, H, N) analyses.

The FT-IR spectra of compounds **2a, 3a** and **4a** displayed two distinct bands in the ranges of 3422-3117 and 3405-3070 cm^{-1}, corresponding to NH_2 group. Additionally, all IR spectra exhibited characteristic bands in the range of 1715-1625 cm^{-1}, which attributed to the C=O amide groups. In the ^{1}H NMR spectra, the compounds showed specific signals corresponding to their unique structures. For instance, 2,5-dioxoimidazo[1,2-f]pyrimidin-3-yl)acetamide (**2a**) displayed a doublet of doublets at 4.81 ppm, while 8-oxo-3*H*-imidazo[1,2-g]purin-7-yl)acetamide (**3a**) and 4,7-dioxo-3*H*-imidazo[2,1-e]purin-8-yl)acetamide (**4a**) exhibited triplets at 5.49 ppm and 5.32 ppm, respectively. These signals corresponds to the proton of the $CH_{imidazole}$ group. The methylene group (CH_2) protons appeared as doublets of doublets in the ranges of 2.20-3.15 ppm and 2.38-3.28 ppm, respectively. The electrospray ionization (ESI) mass spectra of the synthesized compounds displayed peaks at *m/z* $[M+1]^+$, which correspond to the molecular mass of the $[M+H]^+$ ion.

Scheme 2 shows the suggested mechanism for the formation of quinoxalinone derivatives **(1a-k).** Initially,

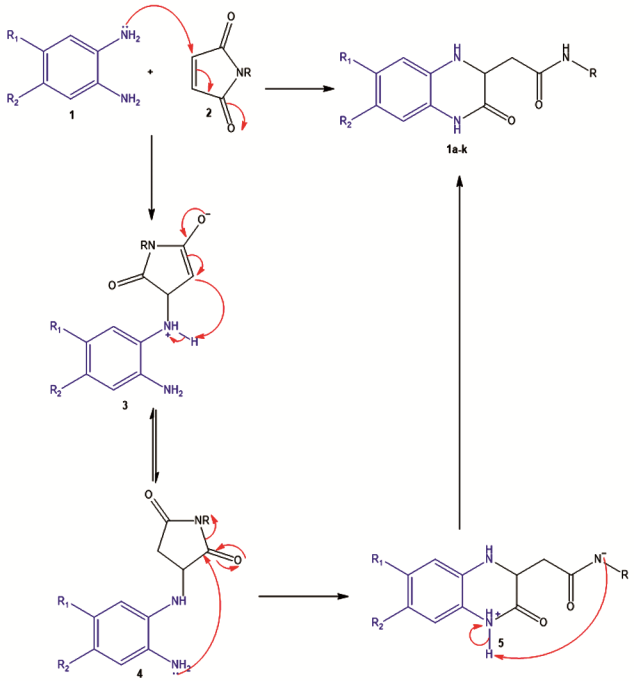

Scheme 2 — Detailed mechanism for the synthesis of **1a-k**

the primary amine (**1**) undergoes nucleophilic addition onto maleimide (**2**) to form intermediate (**3**), which then tautomerizes to yield compounds (**4**). Intramolecular cyclization of compound (**4**) produces intermediates (**5**). Finally, the desired quinoxalinone derivatives **(1a-k)** are obtained through the neutralization of compound (**5**).

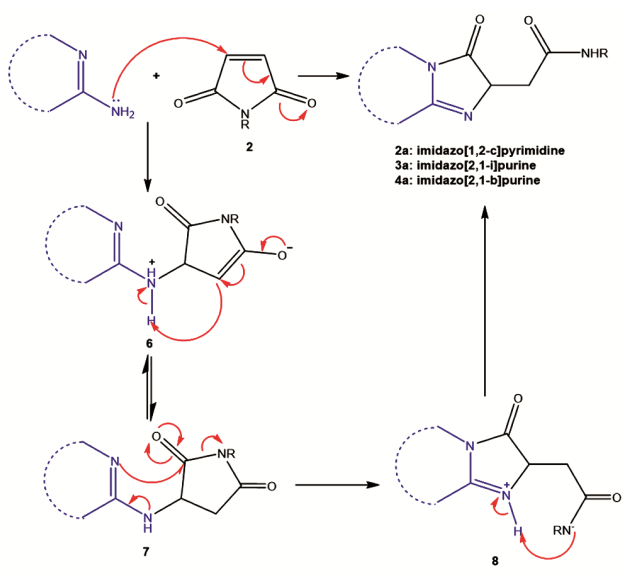

Scheme 3 — Detailed mechanism for the synthesis of product **2a**, **3a**, and **4a**

The formation of compounds **2a**, **3a**, and **4a** follows a mechanism similar to that of the quinoxalinones (**1a-k**), as outlined in Scheme 3. The reaction begins with the nucleophilic attack of the amino group (-NH_2) of nucleobase (adenine, guanine, or cytosine) on the maleimide double bond as electrophelic sites, leading to the formation of a Michael adduct (intermediate **6**). This intermediate then undergoes tautomerization to yield compound (**7**). The imidazole core is formed in compound (**8**) *via* intramolecular cyclization of compound (**7**). Finally, compound (**8**) undergoes neutralization to produce the target compounds **2a**, **3a**, and **4a**.

Biological evaluation

Antioxidant capacity of the prepared compounds

The abilities of the quinoxalinones (**1a-k**), (2,5-dioxoimidazo[1,2-f]pyrimidin-3-yl)acetamide (**2a**), 8-oxo-3*H*-imidazo[1,2-g]purin-7-yl)acetamide (**3a**) and 4,7-dioxo-3*H*-imidazo[2,1-e]purin-8-yl)acetamide (**4a**) to scavenge free radicals were investigated using $DPPH^{\bullet}$ and $ABTS^{+\bullet}$ radical scavenging, and total antioxidant capacity method.

DPPH and ABTS radical scavenging assay

The scavenging activities of the evaluated products are summarized in Table 1, Table 2, and Fig. 1. Overall, the results indicated that all tested compounds exhibited varying degrees of antioxidant effectiveness against both DPPH and ABTS radicals when compared to the standard agent, ascorbic acid.

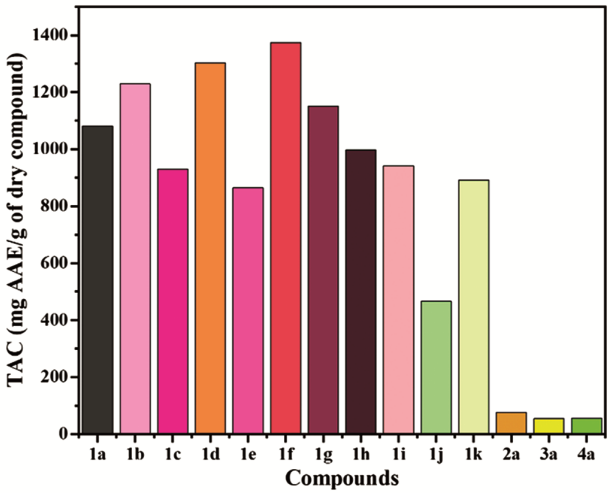

Fig. 3 — IC_{50} values of synthesized compounds by DPPH and ABTS assays

As shown in Fig. 3, the IC_{50} values for the DPPH and ABTS quenching assays ranged from 1.67–17.70 μg $mL^{-1}$and 20.76–218.89 μg mL^{-1}, respectively. These findings indicate that quinoxalinone **1f** exhibited the highest antioxidant activity among all the tested compounds. This product showed IC_{50} values of 1.67 μg mL^{-1} (DPPH) and 20.76 μg mL^{-1} (ABTS), compared to ascorbic acid (IC_{50} = 2.82 μg mL^{-1} for DPPH and 74.22 μg mL^{-1} for ABTS). This significant activity can likely be attributed to the presence of two halogen (Cl) as electron donating group (EDG) in the molecule. These halogen groups can affect the electronic properties of the molecule, potentially enhancing its ability to donate electrons or hydrogen atoms, which are key mechanisms in radical scavenging.

In the case of ABTS experiment, compound **2a** exhibited excellent antioxidant activity, with an IC_{50} value of 73.89 μg mL^{-1}, which is slightly lower than that of the standard ascorbic acid (74.22 μg mL^{-1}).

On the other hand, the lowest antioxidant activity against DPPH radicals was observed in compound **1i**, with an IC_{50} value of 17.69 μg mL^{-1}, compared to ascorbic acid (IC_{50} = 2.82 μg mL^{-1}). Similarly, in the ABTS assay, compound **1c** showed a reduced capacity to scavenge ABTS radicals, with an IC_{50} value of 218.89 μg mL^{-1}, compared to ascorbic acid (IC_{50} = 74.22 μg mL^{-1}).

Interestingly, no detectable antioxidant activity against DPPH radicals was observed in compounds **2a**, **3a**, and **4a**. This lack of activity may be due to oxidative damage to the cytosine, adenine and guanine nuclei by hydroxyl radicals (·OH), which can

alter the structure of pyrimidine nucleobases. These structural changes likely explain the absence of measurable IC_{50} values for these compounds[56-58].

Total antioxidant capacity (TAC)

Fig. 2 illustrates the TAC, represented as milligrams of ascorbic acid equivalent (mg AAE) per gram (g) of sample. The results varied significantly, with quinoxalinones (**1a–k**) showing values ranging from 466 to 1303 mg AAE/g, while the newly synthesized fused imidazo-pyrimidine (**2a**) and imidazo-purine (**3a** and **4a**) compounds exhibited lower values, ranging from 54 to 75 mg AAE/g.

The highest TAC was observed in quinoxalinone **1f**, with a value of 1303 mg AAE/g of dry compound, while the lowest activity was detected in **1j**, with a value of 466 mg AAE/g. Compounds **1d**, **1b**, **1g**, and **1a** demonstrated TAC values of 1303, 1229, 1150, and 1081 mg AAE/g, respectively, which were higher than those of quinoxalinones **1h**, **1i**, and **1c** (997, 941, and 930 mg AAE/g, respectively). Compounds **1e** and **1k** showed similar total antioxidant activities, with values of 864 and 891 mg AAE/g, respectively.

Among the newly synthesized fused heterocycles, imidazo-pyrimidine **2a** exhibited the highest total antioxidant activity, with a TAC of 75 mg AAE/g, surpassing that of imidazo-purines **3a** and **4a** (56 and 54 mg AAE/g, respectively).

Antimicrobial activity

The *in vitro* antibacterial properties of the synthesized compounds were screened against Gram-negative bacteria *Escherichia coli* ATCC 25922, *Klebsiella pneumoniae* ATCC 13883 and *Pseudomonas aeruginosa* ATCC 27853, as well as Gram-positive bacterium *Staphylococcus aureus* ATCC 25923. Additionally, their antifungal activity against *Candida albicans* ATCC 14053 was assessed by the agar well diffusion assay[55] at a concentration of 15 mg/mL. The findings of the antifungal and antibacterial activities were compared with positive controls Nystatin and Gentamicin, respectively. The results are summarized in Table 3.

From the findings in Table 3, most of the synthesized quinoxalinones exhibited significant zones of inhibition against both G^- and G^+ bacteria. The highest antibacterial activity was observed for compound **1f** against *S. aureus*, with a zone of inhibition (ZOI) diameter of 20 mm, compared to gentamicin (21 mm). The imidazo[1,2-c]pyrimidine **2a** showed moderate activity, with a ZOI diameter of 11 mm against *K. pneumoniae*. In contrast, none of the tested imidazo-purine derivatives (**3a** and **4a**) demonstrated bactericidal effects.

Regarding antifungal activity, the results indicated that several compounds exhibited significant potency against the tested *C. albicans* strain. Compound **1f** displayed the strongest antifungal activity, with a ZOI diameter of 20 mm, compared to nystatin (24 mm). Compound **1b** showed limited effectiveness against the fungal strain, with a ZOI diameter of 7 mm at a concentration of 15 mg/mL. On the other hand, imidazo[1,2-c]pyrimidine (**2a**), imidazo[2,1-i]purine (**3a**), and imidazo[2,1-b]purine (**4a**) showed no antifungal activity.

Conclusion

In brief, a variety of newly synthesized fused compounds, specifically quioxalinones, imidazo [1,2-c]pyrimidine acetamide, imidazo [2,1-i]purine acetamide, and imidazo [2,1-b]purine acetamide, were effectively produced by the condensation of maleimide with substituted *o*-phenylenediamines or nucleobases in ethanol as the solvent. The antioxidant potential of the synthesized compounds was evaluated using DPPH, ABTS, and TAC assays. In addition, the antimicrobial properties of these compounds was conducted against four bacterial strains, namely *E. coli*, *K. pneumoniae*, *P. aeruginosa*, and *S. aureus*, and against one fungal strain, *C. albicans*, using the well-diffusion method. The findings of this study demonstrate that the synthesized heterocyclic compounds exhibit significant antioxidant and antimicrobial activities, with compound **1f** showing the strongest potential across both assays. The observed antioxidant properties, indicated by a notable reduction in radical scavenging and TAC, suggest that quinoxalinone **1f** and imidazo-pyrimidine **2a** could be valuable in the development of drugs aimed at combating oxidative stress-related diseases. Furthermore, the promising antimicrobial activity of compound **1f**, particularly against *S. aureus* and *C. albicans* strains, highlights its potential for use in treating infections caused by resistant pathogens.

Supplementary Information

Supplementary information is available in the website https://nopr.niscpr.res.in/handle/123456789/58776.

Acknowledgement

The authors are grateful to the Algerian Ministry of Higher Education and Scientific Research and the

General Directorate for Scientific Research and Technological Development (DGRSDT) for its financial support under PRFU project no. B00L01UN-390120230001.

References

1 Majee S, Shilpa, Sarav M, Banik B K & Ray D, *Pharmaceuticals*, 16 (2023) 873.
2 Dinodia M, *Mini-Rev Org Chem*, 20 (2023) 155.
3 Heravi M M & Zadsirjan V, *RSC Adv*, 10 (2020) 44247.
4 Ruzi Z, Nie L, Bozorov K, Zhao J & Aisa H A, *Arch Pharm,*354 (2021) 2000470.
5 Khabnadideh S, Rezaei Z, Khalafi-Nezhad A, Bahrinajafi R, Mohamadi R & Farrokhroz A A, *Bioorg Med Chem Lett*, 13 (2003) 2863.
6 Nascimento M V P, Munhoz A C, Theindl L C, Mohr E T B, Saleh N, Parisotto E B, Rossa T A, Zamoner A, Creczynski-Pasa T B, Filippin-Monteiro F B & Sá M M, *Inflamm*, 41 (2018)1334.
7 Sharma D, Narasimhan B, Kumar P, Judge V, Narang R, De Clercq E & Balzarini J, *Eur J Med Chem*, 44 (2009) 2347.
8 Łażewska D, Więcek M, Ligneau X, Kottke T, Weizel L, Seifert R, Schunack W, Stark H & Kieć-Kononowicz K, *Bioorg Med Chem Lett*, 19 (2009) 6682.
9 Sánchez-Moreno M, Gómez-Contreras F, Navarro P, Marín C, Ramírez-Macías I, Olmo F, Sanz AM, Campayo L, Cano C & Yunta M J, *J Antimicro Chemo,* 67 (2012) 387.
10 Stover C K, Warrener P, VanDevanter D R, Sherman D R, Arain T M, Langhorne M H, Anderson S W, Towell J A, Yuan Y, McMurray D N & Kreiswirth B N, *Nat*, 405 (2000) 962.
11 Ratanlal M, Mohankrishnan D, Jayaram V, Sahal D & Sharma G V, *Chem Sel,* 9 (2024) 202302636.
12 Kumar P, Syal, B, Seboletswe P, Cele N, Olofinsan K, Singh P, Shahidul Islam M, Singh D & Gupta P, *Chem Sel,* 8 (2023) 202300924.
13 Galley G, Stalder H, Goergler A, Hoener, M C & Norcross R D, *Bioorg Med Chem Lett,* 22 (2012) 5244.
14 Hancock A A, Bennani,Y L, Bush E N, Esbenshade T A, Faghih R, Fox G B & Yao B B, *Eur J Pharm,* 487 (2004) 183.
15 Carini D J, Duncia J V, Aldrich P E, Chiu A T, Johnson A L, Pierce M E, Price W A, Santella III J B & Wells G J, *J Med Chem,* 34 (1991) 2525.
16 Kilic-Kurt Z, Ozmen N & Bakar-Ates F, *Bioorg Chem,* 101 (2020) 104028.
17 Hassan A Y, Sarg M T, Bayoumi A H & Kalaf F G A, *J Heterocycl Chem,* 54 (2017) 3458.
18 Gujjarappa R, Kabi A K, Sravani S, Garg A, Vodnala N, Tyagi U, Kaldhi D, Velayutham R, Singh V, Gupta S & Malakar C C, *In Nanostructured Biomaterials: Basic Structures and Applications,* (Springer Singapore, Singapore) 2022, p. 135.
19 Serdaliyeva D, Nurgozhin T, Satbayeva E, Khayitova M, Seitaliyeva & Ananyeva L, *J Clin Med Kaz,* 19 (2022) 11.
20 Verma P, Pal S, Chauhan S, Mishra A, Sinha I, Singh S & Srivastava V, *J Mol Struct,* 1023 (2020) 27410.
21 Kim M H, Jung S Y, Song K H, Park J I, Ahn J, Kim E H, Park J K, Hwang S G, Woo H J & Song J Y, *J Cell Mol Med,* 24 (2020) 830.
22 Dhiman P, Malik N, Verma P K & Khatkar A, *Res Chem Intermed,* 41 (2015) 8699.
23 Abdel-Mohsen H T, Abood A, Flanagan K J, Meindl A, Senge M O & El Diwani H I, *Arch Pharm,* 353 (2020)1900271.
24 Mosselhi M A, Darwish E S & Peseke K, *Monatsh Chem,* 139 (2008) 825.
25 Abdelall E K, Abdelhamid A O & Azouz A A, *Bioorg Med Chem Lett*, 27 (2017) 4358.
26 Drabczyńska A, Müller C E, Karolak-Wojciechowska J, Schumacher B, Schiedel A, Yuzlenko O & Kieć-Kononowicz K, *Bioorg Med Chem,* 15 (2007) 5003.
27 Solomyannyi R, Mitiukhin O, Prichard M, James S, Hartline C, Zhirnov V & Brovarets V, *Curr Chem Lett,* 9 (2020) 89.
28 Alqarni S, Cooper L, Galvan Achi J, Bott R, Sali V K, Brown A, Santarsiero B D, Krunic A, Manicassamy B, Peet N P & Zhang P, *J Med Chem,* 65 (2022) 14104.
29 Amblard F, Fromentin E, Detorio M, Obikhod A, Rapp K L, McBrayer T R, Whitaker T, Coats S J & Schinazi R F, *Eur J med Chem,* 44 (2009) 3845.
30 Almirante L, Polo L, Provinciali E, Rugarli P, Gamba A, Olivi A & Murmann W, *J Med Chem,* 9 (1966) 29.
31 Goodacre S C, Street L J, Hallett D J, Crawforth J M, Kelly S, Owens A P, Blackaby W P, Lewis R T, Stanley J, Smith A J & Ferris P, *J Med Chem,* 49 (2006) 35.
32 Drabczyńska A, Müller C E, Lacher S K, Schumacher B, Karolak-Wojciechowska J, Nasal A, Kawczak P, Yuzlenko O, Pękala E & Kieć-Kononowicz K, *Bioorg Med Chem,* 14 (2006) 7258.
33 Fang Y Q, Zhang H J, Ren Y& Quan Z S, *Lat Am J Pharm,* 37 (2018) 170.
34 Zagórska A, Partyka A, Bucki A, Kołaczkowski M, Jastrzębska-Więsek M, Czopek A, Siwek A, Głuch-Lutwin M, Bednarski M, Bajda M & Jończyk J, *Chem Biol Drug Des,* 93 (2019) 511.
35 Prasad P, Kalola A G & Patel M P, *New J Chem,* 42 (2018) 12666.
36 Jaromin A, Zagórska A, Parapini S, Basilico N & Gubernator J, *New 5-HT1A receptor ligands as promising inhibitors of the growth of Plasmodium falciparum,* (Basel, Switzerland) 2020.
37 Peytam F, Takalloobanafshi G, Saadattalab T, Emamgholipour Z, Norouzbahari M, Moghimi S, Firoozpour L, Bijanzadeh H R, Faramarzi M A, Mojtabavi S & Rashidi-Ranjbar P, *Res Sq,* (2021) 1.
38 Mahmoodi N O, Rahimi S & Nadamani M P, *Dyes Pigm,* 143 (2017) 387.
39 Rao R N, Mm B, Maiti B, Thakuria R & Chanda K, *ACS Comb Sci,* 20 (2018) *20,* 164.
40 Anamika, Yadav C L, Drew M G, Kumar K & Singh N, *Inorg Chem,* 60 (2021) 6446.
41 Ramírez-Trinidad Á, Carrillo-Jaimes K, Rivera-Chávez J A & Hernandez-Vazquez E, *Med Chem Res,* 32 (2023) 144.
42 Grazia Martina M, Giannessi L& Radi M, *Eur J Org Chem,* 26 (2023) 202201288.
43 Merroun Y, Chehab S, Hallaoui A E, Boukhris S, Ghailane & Souizi A, *Rev Chem Intermed,* 50 (2024) 1.
44 Pestov A V, Privar Y O, Mekhaev A V, Fedorets A N, Ezhikova M A, Kodess M I & Bratskaya S Y, *Eur Poly J,* 115 (2019) 356.

45 Azzouzi M, El Ouafi Z, Azougagh O, Daoudi W, Ghazal H, El Barkany S, Abderrazak R, Mazières S, El Aatiaoui A & Oussaid A, *J Mol Struc,* 1285 (2023) 135525.
46 Baranwal J, Singh S, Kushwaha S & Jyoti A, *Lett Org Chem,* 20 (2023) 446.
47 Genç Y, Özkanca R & Bekdemir Y, *Ann Clin Microbio Antimicro,* 7 (2008) 1.
48 Reddyrajula R & Dalimba U K, *New J Chem,* 43 (2019) 16281.
49 Boukhallout F E, Dehamchia M, Bayou S, Adaika C, Mohammed A M & Régaïnia Z, *Ind J Hetero Chem,* 34 (2024) 421.
50 Bayou-Khier N, Benchikha N, Amari M & Hammadi M, *J Fund Appl Sci,* 11 (2019) 1256.
51 Rozhkov S S, Ovchinnikov K L & Kolobov A V, *Russ Chem Bull,* 63 (2014) 137.
52 Cetin A & Geçibesler I H, *J App Pharm Sci,* 5 (2015) 120.
53 Re R, Pellegrini N, Proteggente A, Pannala A, Yang M & Rice-Evans C, *Free Radic Boil Med,* 26 (1999) 1231.
54 Prieto P, Pineda M & Aguilar M, *Anal Biochem,* 269 (1999) 337.
55 Jahangirian H, Haron M J, Shah M H, Abdollahi Y, Rezayi M & Vafaei N, *Digest J Nanomat Biostruc,* 8 (2013) 1263.
56 Favier A, *L'act Chim,* 108 (2003) 863.
57 Borràs V J, Francés-Monerris A & Roca-Sanjuán D, *Chem Photo Chem,* 3 (2019) 889.
58 Singh A, Kukreti R, Saso L & Kukreti S, *Int J Mol Sci,* 20 (2019) 4258.